Intermetallics 69 (2016) 118–122

Contents lists available at ScienceDirect

Intermetallics

journal homepage: www.elsevier.com/locate/intermet

Magneto-structural transition and magnetocaloric effect of melt spinning $Ni_{50}Mn_{29}Ga_{21-x}Tb_x$ (x = 0-1) ribbons

Yuye Wu, Xiao Wang, Jingmin Wang*, Chengbao Jiang**, Huibin Xu

Key Laboratory of Aerospace Materials and Performance (Ministry of Education), School of Materials Science and Engineering, Beihang University, Beijing 100191, PR China

ARTICLE INFO

Article history:
Received 28 July 2015
Received in revised form
16 September 2015
Accepted 8 October 2015
Available online 14 November 2015

Keywords:
A. Functional alloys
B. Magnetic properties
B. Martensitic transformations

ABSTRACT

$Ni_{50}Mn_{29}Ga_{21-x}Tb_x$ (x=0-1) ribbons with the solid solution of Tb element were synthesized by the melt spinning method. The phase transformation, magnetic properties and magnetocaloric effect were investigated. With the increasing Tb content the martensitic transformation temperatures were gradually increased while the Curie temperature was monotonously decreased. According to the detected phase transition temperatures, a phase diagram was established to describe the dependence of the magneto-structural transition on the Tb content. Three types of magneto-structural transitions were observed. Especially, the martensitic transformation was coincided with the magnetic transition in the single phase alloy with x = 0.1, giving rise to the coupled magneto-structural transition from ferromagnetic martensite to paramagnetic austenite. Sizable magnetic entropy change of 4.31 J/Kg K was induced from the coupled magneto-structural transition by the application of magnetic field of 50 kOe at 349.5 K.

1. Introduction

The magnetocaloric effect (MCE) of materials have attracted considerable attentions since Brown discovered that magnetocaloric materials can be successfully applied for magnetic refrigeration [1]. Up to date, giant magnetic entropy changes (ΔS_M) which features the large MCE have been obtained in several alloy systems undergoing the first-order magneto-structural transition, such as La–Fe–Si [2–5], Gd–Si–Ge [6–8] and Mn–As(-Sb) [9,10] etc. In recent years, the Heusler-type Ni–Mn-based ferromagnetic shape memory alloys (FSMAs), have emerged as a new type of magnetocaloric materials. Large MCE has been discovered in the Ni–Mn-based alloys possessing coupled magneto-structural transition [11–13]. For Ni–Mn–X (X = In, Sn, Sb) alloys, large reverse MCE has been realized from the magneto-structural transition from weak magnetic martensite to ferromagnetic austenite [11,14–17]. For the typical Ni–Mn–Ga alloys and the recently developed Ni–Mn–Ti alloys, large direct MCE can be induced from the magneto-structural transition from ferromagnetic martensite to paramagnetic austenite [18,19]. It has been confirmed that doping the fourth elements is an effective way to tune the magneto-structural transition and the MCE of Ni–Mn-based alloys. Until now, the added fourth elements are mainly focused on the *3d* elements, such as Co, Cu and Fe, etc [20–24]. Recently it has been reported that the phase transition temperatures can also be manipulated by the addition of rare earth (RE) elements [25–33]. It was found that the solid solubility of the large size RE atoms were quite low in the as-cast alloys due to the low solidification rate [26,28,31]. Therefore, the micron-sized RE-rich precipitates are formed in the as-cast samples and the matrix is still kept as ternary Ni–Mn–Ga compositions. Recently, we found that by adopting the rapid solidification method, the solid solubility of RE elements in Ni–Mn–Ga alloys was increased [34]. However, it remains unclear whether there is the coupled magneto-structural transition and the MCE in the rapidly solidified Ni–Mn–Ga–RE alloys. In this paper, $Ni_{50}Mn_{29}Ga_{21-x}Tb_x$ (x=0-1) ribbons are synthesized by melt spinning method. The compositional dependence of the temperature of both martensitic transition and magnetic transitions are studied. Consequently, a phase diagram describing the relationship between the composition and the magneto-structural transitions is established. The coupled magneto-structural transition from ferromagnetic martensite to paramagnetic austenite is observed in the $Ni_{50}Mn_{29}Ga_{20.9}Tb_{0.1}$ ribbon. Sizeable magnetic entropy change

* Corresponding author.
** Corresponding author.
E-mail addresses: jingmin@buaa.edu.cn (J. Wang), jiangcb@buaa.edu.cn (C. Jiang).

http://dx.doi.org/10.1016/j.intermet.2015.10.004
0966-9795/

is induced by the magnetic field in the vicinity of the coupled magneto-structural transition. This work may put new insight into the understanding of the phase transition and MCE of Ni–Mn-based alloys.

2. Experimental methods

High-purity nickel, manganese, gallium and terbium with a purity level of 99.9%, 99.7%, 99.99% and 99.99%, respectively, were arc-melted four times into buttons for the preparation of $Ni_{50}Mn_{29}Ga_{21-x}Tb_x$($x$ = 0-1) master alloys. The ingots were encapsulated in a quartz tube filled with argon, heat treated at 1123 K for 48 h for homogenization, and quenched into cold water. Subsequently, the ingots were induction melted in a quartz tube and melt spinning in vacuum, at a wheel surface line speed of 20 m/s. Ribbons with the width of 3 mm and length of 25–35 mm were obtained. METTLER Toledo differential scanning calorimetry (DSC) was used to determine the martensitic transformation temperatures with the heating and cooling rate of 10 K/min. The field dependent magnetization (*M-H*) and the temperature dependent magnetization (*M-T*) curves were measured on the physical properties measurement system (PPMS). The magnetic entropy change caused by magnetic field was estimated according to the measured isothermal *M-H* curves.

3. Results and discussions

Fig. 1 shows the DSC and *M-T* curves of $Ni_{50}Mn_{29}Ga_{21-x}Tb_x$ (x = 0-1) ribbons. The first-order martensitic transformation is detected over the whole composition range, as evidenced by the endothermic peak on heating and the exothermic peak on cooling of the DSC curves. The martensitic transformation temperatures, including the austenitic starting and finishing temperatures A_s and A_f, the martensitic starting and finishing temperatures M_s and M_f are determined from the DSC curves, as indicated in Fig. 1(a). The second-order magnetic transition from ferromagnetism to paramagnetism is confirmed by the *M-T* curves measured under the magnetic field of 500 Oe. The Curie temperature T_C is taken as the temperature where the differential dM/dT reaches the minimum value, as shown in the insets. Upon heating, the magnetization exhibited a slow increase first and then a sharp or slight fall around T_C. The *M-T* curves around T_C show quite different shape for the ribbons with different Tb content. The reasons will be discussed later.

According to the relative relationship between the temperatures of the martensitic transformation and the magnetic transition, the presently studied ribbons are divided into three categories, as shown in Fig. 1. For the ternary ribbon with $x = 0$, T_C is determined to be 359.2 K and A_f is 351.8 K, that is $A_f < T_C^A$, as shown in Fig. 1(a) This means that the magnetic transition takes place after the martensitic transformation. For the ribbon with $x = 0.1$, it is interesting to find that T_C is located between A_s and A_f, as shown in Fig. 1(b). This implies that the structural martensitic transformation coincides with the magnetic transition. For the ribbons with $x \geq 0.2$, as shown in Fig. 1(c), the reverse martensitic transformation starting temperature A_s is confirmed to be 365.7 K, 367.9 K and 372.6 K, and T_C^M is 352.5 K, 346.7 K and 335.3 K for $x = 0.2$, 0.5 and 1, respectively. Obviously $T_C^M < A_s$, hence the magnetic transition occurs before the martensitic transformation. Therefore, the different slopes of *M-T* curves near T_C can be explained based on the transition sequences. For the ribbons with $x = 0$ and 0.1, the abrupt fall of the magnetization is attributed to the partial or complete coincidence of the martensitic and magnetic transitions. While for the ribbons with $x \geq 0.2$, the slight decrease of the magnetization on heating is simply from the magnetic transition of the martensite

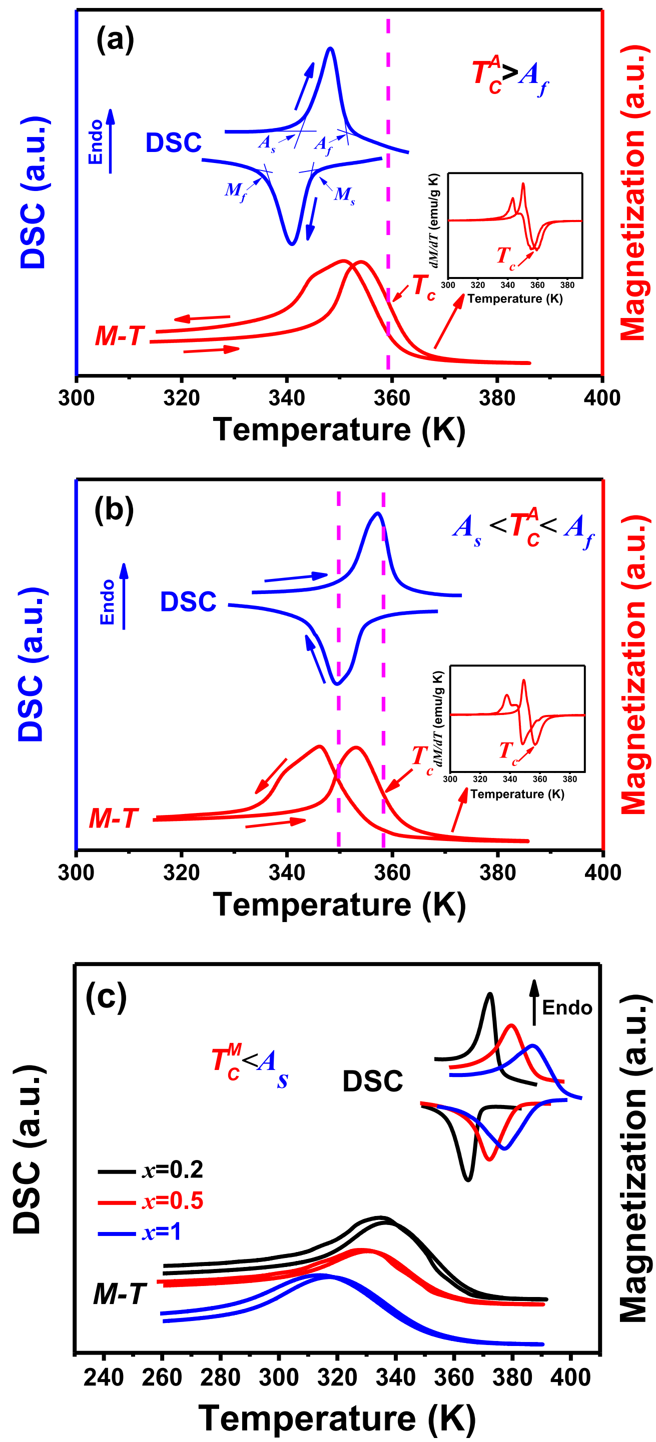

Fig. 1. DSC and *M-T* curves of $Ni_{50}Mn_{29}Ga_{21-x}Tb_x$ ribbons with (a) $x = 0$, (b) $x = 0.1$ and (c) $x = 0.2$-1. The insets in (a) and (b) are the corresponding differential curves of the *M-T* curves.

phase with lower symmetry compared with the austenite phase.

Based on the determined transition temperatures, a vertical section phase diagram is established for the presently studied $Ni_{50}Mn_{29}Ga_{21-x}Tb_x$ (x = 0-1) ribbons, as plotted in Fig. 2. It is found that with the increasing Tb content, the martensitic transformation temperatures are monotonously increased but the Curie temperature is gradually decreased. Generally, the martensitic transition temperature of Ni–Mn based Heusler alloys is sensitive to the